Electronic Supplementary Material (ESI) for Sustainable Energy & Fuels.

Converting micro-sized kerf-loss silicon waste to high-performance hollow-structured silicon/carbon composite anodes for lithium-ion batteries

Qiang Ma[a], Jiakang Qu[a], Xiang Chen[a], Zhuqing Zhao[a], Yan Zhao[a], Haijia Zhao[a], Hongwei Xie[a], Pengfei Xing*[a], Huayi Yin*[a,b]

a. Key Laboratory for Ecological Metallurgy of Multimetallic Mineral of Ministry of Education, School of metallurgy, Northeastern University, Shenyang 110819, P. R. China.
b. Key Laboratory of Data Analytics and Optimization for Smart Industry, Ministry of Education, Northeastern University, Shenyang 110819, P. R. China.
*Corresponding author. Email: yinhy@smm.neu.edu.cn (Huayi Yin) Email: xingpf@smm.neu.edu.cn (Pengfei Xing)

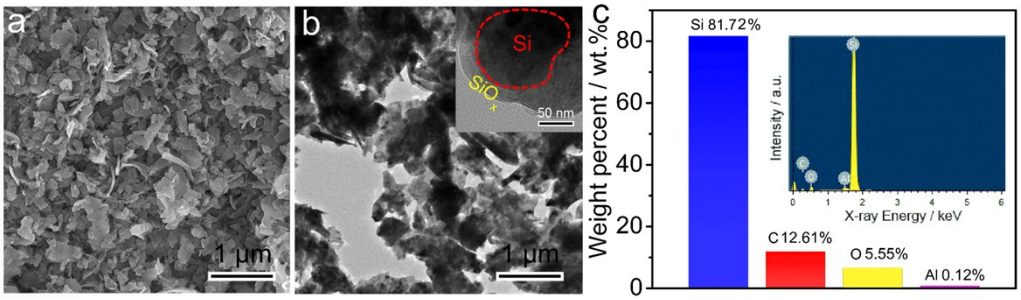

Fig. S1 (a) SEM and (b) TEM images of KL-Si. (c) EDS analysis with displaying weight percent of elements in the KL-Si.

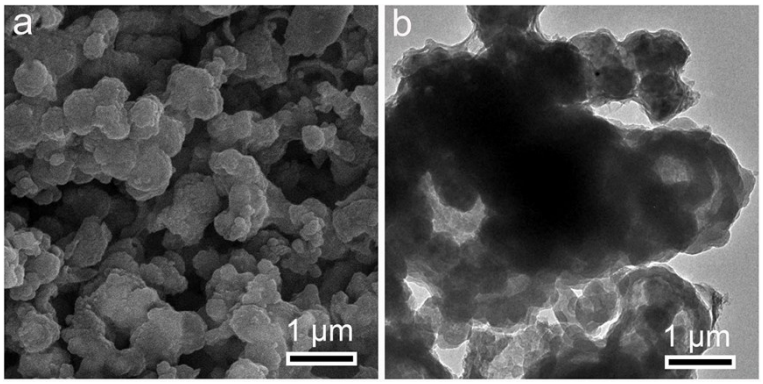

Fig. S2 (a) SEM and (b) TEM images of KL-Si@C

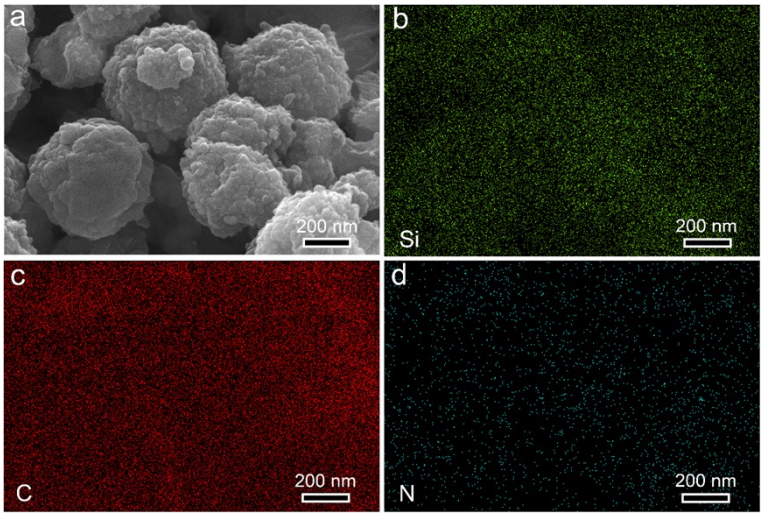

Fig. S3 (a) SEM image Si@void@C, corresponding Si (b), C (c), N (d) elemental mapping images.

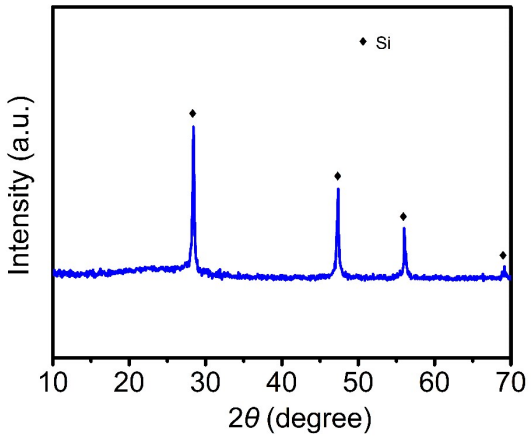

Fig. S4 XRD pattern of after etching KL-Si in HF solution.

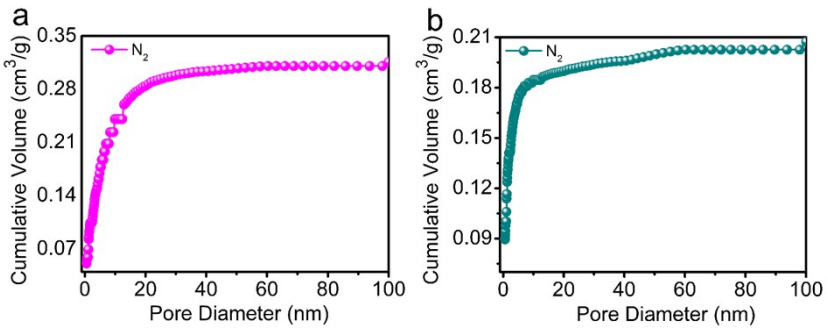

Fig. S5 Cumulative-desorption pore volume distribution curves of (a) Si@void@C, and (b) KL-Si@C.

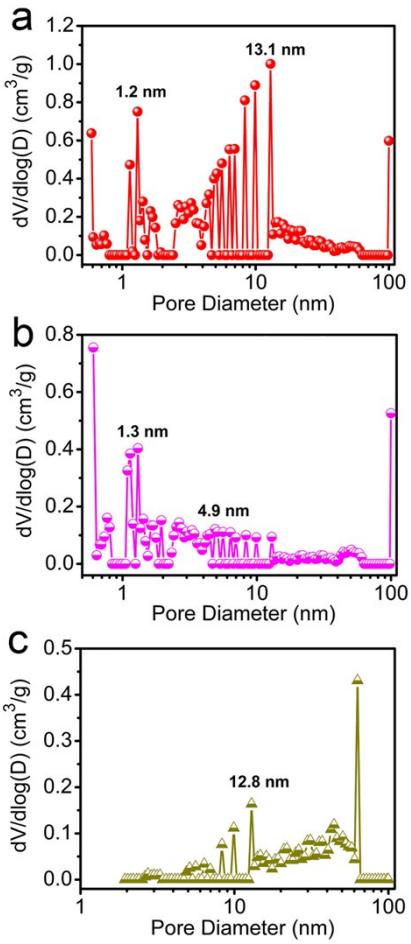

Fig. S6 Pore size distribution of the (a) Si@void@C, (b) KL-Si@C, and (c) KL-Si.

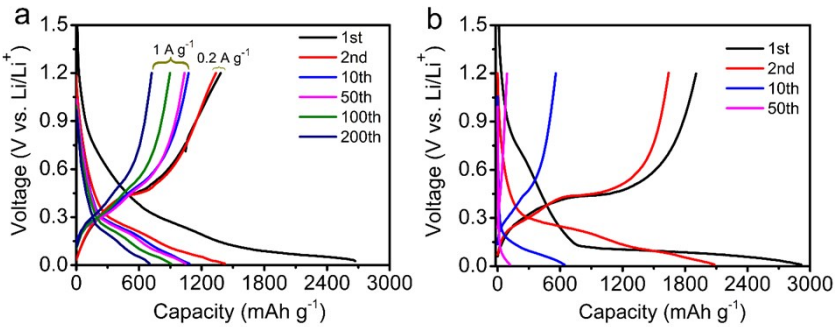

Fig. S7 Galvanostatic charge/discharge profiles of (a) KL-Si@C and (b) KL-Si at each current density from 0.2 to 1 A g^{-1}, respectively.

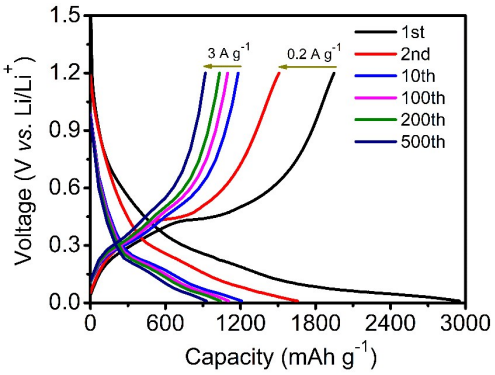

Fig. S8 Galvanostatic charge/discharge profile of Si@void@C at each current density from 0.2 to 3 A g^{-1}.

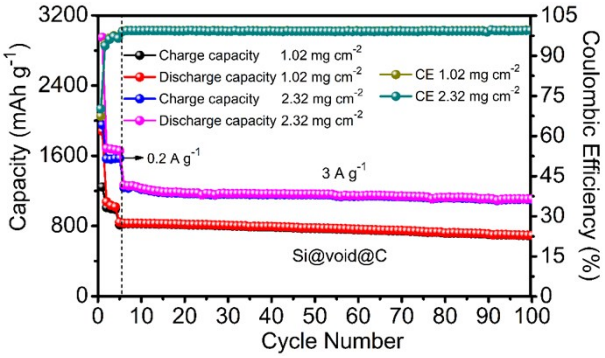

Fig. S9 Discharge capacities *vs*. cycling number of the Si@void@C anode with different mass loadings at 3 A g^{-1} (the initial three cycles are carried out at 0.2 A g^{-1}).

Table S1. Surface areas and pore structures of KL-Si, KL-Si@C, and Si@void@C

Samples	BET analysis						
	S_{BET} ($m^2 g^{-1}$)	S_{micro}[a] ($m^2 g^{-1}$)	S_{meso}[b] ($m^2 g^{-1}$)	V_{total}[c] ($cm^3 g^{-1}$)	V_{micro}[d] ($cm^3 g^{-1}$)	V_{meso}[e] ($cm^3 g^{-1}$)	D_{aver} (nm)
KL-Si	19.11	3.48	13.07	0.07	0.002	0.067	14.6
KL-Si@C	317.29	208.88	94.35	0.21	0.11	0.099	2.6
Si@void@C	333.25	116.29	176.26	0.33	0.06	0.26	4.2

[a]S_{micro} is the surface area of the micropores. [b]S_{meso} is the surface area of the mesopores. [c]V_{total} is the total pore volume. [d]V_{micro} is the volume of the micropores. [e]V_{meso} is the volume of the mesopores.

Table S2. Equivalent series resistance (R_e) and charge transfer resistance (R_{ct}) of the KL-Si, KL-Si@C, and Si@void@C.

Samples	$\boldsymbol{R_e}$ **(Ω)**	$\boldsymbol{R_{ct}}$ **(Ω)**
KL-Si	10.37	117.73
KL-Si@C	9.18	75.02
Si@void@C	8.41	56.31

Table S3. Comparison of the electrochemical performance of the as-prepared samples with other Si-based anode materials for lithium-ion battery.

Materials	Si content	Tests done at/Initial discharge specific capacity	Cycling performance	Ref.
			Tests done at/Cycle number/Specific capacity	
Core-shell structured nano-Si/C	81 wt.%	0.1 (A g^{-1})/~2300 mAh g^{-1}	0.1 (A g^{-1})/50/~1800 mAh g^{-1}	1
Micro-nano Si/SiO_x/PAN	80 wt.%	0.1 (A g^{-1})/2734 mAh g^{-1}	0.1 (A g^{-1})/100/988 mAh g^{-1}	2
Nanoarchitecture Si/C	87 wt.%	0.12 (A g^{-1})/2505 mAh g^{-1}	1.2 (A g^{-1})/500/1150 mAh g^{-1}	3
Mesoporous Si@C microspheres	32 wt.%	0.05 (A g^{-1})/1637 mAh g^{-1}	0.05 (A g^{-1})/100/1053 mAh g^{-1}	4
yolk-shell structure Si/C	71 wt.%	0.4 (A g^{-1})/2833 mAh g^{-1}	0.4 (A g^{-1})/50/~2000 mAh g^{-1}	5
core-shell Si/C fibers	22 wt.%	0.2 (A g^{-1})/~1600 mAh g^{-1}	0.5 (A g^{-1})/300/603 mAh g^{-1}	[6]
Core-shell fibers Si/C	50 wt.%	0.12 (A g^{-1})/1500 mAh g^{-1}	2.75 (A g^{-1})/300/750 mAh g^{-1}	7
Yolk-Shell Porous Si@C	65 wt.%	0.2 (A/g)/1876 mAh g^{-1}	1 (A g^{-1})/600/600 mAh g^{-1}	8
Hollow core-shell structured Si/C	37 wt.%	0.1 (A g^{-1})/1370 mAh g^{-1}	0.1 (A g^{-1})/100/783 mAh g^{-1}	9
Porous Si with N-doped carbon	49 wt.%	0.2 (A g^{-1})/1612 mAh g^{-1}	0.2 (A g^{-1})/200/750 mAh g^{-1}	10
Si/mesoporous carbon	10 wt.%	0.2 (A g^{-1})/1362 mAh g^{-1}	0.2(A g^{-1})/100/581 mAh g^{-1}	11
Mesoporous C/Si composite	76 wt.%	0.2 (A g^{-1})/~2700 mAh g^{-1}	0.5(A g^{-1})/100/1018 mAh g^{-1}	12
Porous Si/C microspheres	44 wt.%	0.2 (A g^{-1})/~1500 mAh g^{-1}	0.2(A g^{-1})/100/~530 mAh g^{-1}	13
Si@void@C	43 wt.%	0.2 (A g^{-1})/2710 mAh g^{-1}	1 (A g^{-1})/300/1164.4 mAh g^{-1} 3 (A g^{-1})/500/927 mAh g^{-1}	This work

References

1 Y. Hwa, W.-S. Kim, S.-H. Hong and H.-J. Sohn, *Electrochim. Acta*, 2012, **71**, 201-205.

2 J. Wang, M. Zhou, G. Tan, S. Chen, F. Wu, J. Lu and K. Amine, *Nanoscale*, 2015, **7**, 8023-8034.

3 F. M. Hassan, V. Chabot, A. R. Elsayed, X. Xiao and Z. Chen, *Nano Lett.*, 2014, **14**, 277-283.

4 X. Ma, M. Liu, L. Gan, P. K. Tripathi, Y. Zhao, D. Zhu, Z. Xu and L. Chen, *Phys. Chem. Chem. Phys.*, 2014, **16**, 4135-4142.

5 N. Liu, H. Wu, M. T. McDowell, Y. Yao, C. Wang and Y. Cui, *Nano Lett.*, 2012, **12**, 3315-3321.

6 H. Zhang, X. Qin, J. Wu, Y.-B. He, H. Du, B. Li and F. Kang, *J. Mater. Chem. A*, 2015, **3**, 7112-7120.

7 T. H. Hwang, Y. M. Lee, B.-S. Kong, J.-S. Seo and J. W. Choi, *Nano Lett.*, 2012, **12**, 802-807.

8 S. Guo, X. Hu, Y. Hou and Z. Wen, *ACS Appl. Mater. Interfaces*, 2017, **9**, 42084-42092.

9 H. Tao, L.-Z. Fan, W.-L. Song, M. Wu, X. He and X. Qu, *Nanoscale*, 2014, **6**, 3138-3142.

10 Y. Xing, L. Zhang, S. Mao, X. Wang, H. Wenren, X. Xia, C. Gu and J. Tu, *Mater. Res. Bull.*, 2018, **108**, 170-175.

11 T. Shen, X.-h. Xia, D. Xie, Z.-j. Yao, Y. Zhong, J.-y. Zhan, D.-h. Wang, J.-b. Wu, X.-l. Wang and J.-p. Tu, *J. Mater. Chem. A*, 2017, **5**, 11197-11203.

12 Y. Xu, Y. Zhu and C. Wang, *J. Mater. Chem. A*, 2014, **2**, 9751-9757.

13 Y. Ru, D. G. Evans, H. Zhu and W. Yang, *RSC Adv.*, 2014, **4**, 71-75.